Desalination and Water Treatment
www.deswater.com

17 (2010) 143–149
May

1944-3994/1944-3986 © 2010 Desalination Publications. All rights reserved
doi: 10.5004/dwt.2010.1710

Superior molecular size screening and mass-transfer characterization of calcium alginate membrane

K. Kashima, M. Imai*, I. Suzuki

Course in Bioresource Utilization Sciences, Graduate School of Bioresource Sciences, Nihon University, 1866 Kameino, Fujisawa, Kanagawa- Pref. 252-8520, Japan
Tel. +81466843978, Fax: +81466843978, email: XLT05104@nifty.com

Received 8 August 2009; accepted 22 November 2009

ABSTRACT

A stable calcium alginate membrane was successfully prepared. The membrane performs a superior molecular size screening between 60 Da (urea) and 60 4Da (Bordeaux S). The effective diffusion coefficient in the membrane was changed 2.5×10^4-fold even when our tested molecular size was only 10-fold. The pore size for mass transfer in the membrane was speculated as being mono-disperse in our experimental molecular size. The membrane has sufficient mechanical strength for conventional use in its swelled state in an aqueous phase. Its polymeric framework of calcium alginate became densely populated with increasing calcium chloride concentration, and its mechanical strength was elevated. This then dominantly influenced the mass transfer tortuosity in the membrane. The water permeation flux was linearly proportional to pressure. The mechanism of water permeation mainly exhibited a Hagen-Poiseuille flow. Pores were not observed at the surface in a scanning-electron-microscope view.

Keywords: Calcium alginate; Membrane; Mass transfer; Effective diffusion coefficient

1. Introduction

The development of a means of utilizing reproducible bioresources is a prospective strategy for ensuring sustainable engineering sciences. Alginic acid is abundantly obtained as a marine biological resource, being especially produced by brown-algae seaweed. Alginates have been widely used in the food industry as thickeners, suspending agents, emulsion stabilizers, gelling agents, and film-forming agents [1].

Sodium alginate is well known as a hydrophilic polysaccharide. It consists of a linear copolymer composed of two monomeric units, 1,4-linked β-D-mannuronic acid, C-5 epimer, and α-L-guluronic acid, in varying proportions (Fig. 1). The physical properties of sodium alginate are very susceptible to changes in chemical factors (pH, total ionic strength, etc.). At near-neutral pH, the high negative charge of sodium alginates due to deprotonated carboxylic functional groups induces repulsive inter- and intra-molecular electrostatic forces. The change in ionic strength in a sodium alginate aqueous solution has a very significant effect, especially on polymer chain extension [2].

Sodium alginate is conveniently formed into a gel structure by the presence of divalent cations such as Ca^{2+}, resulting in a highly compacted gel network [2–4]. It is often employed and investigated as a carrier of immobilized enzyme, a drug delivery capsule, [5] and a food supplement [6–8]. In contrast, alginate membrane has been less investigated. It is supported by glass fiber [9] and is found in hybrids with other polymer materials [10,11].

*Corresponding author

Presented at the Fifth Conference of the Aseanian Membrane Society Aseania 2009 "Recent Progress in Membrane Science and Technology", 12–14 July 2009, Kobe, Japan.

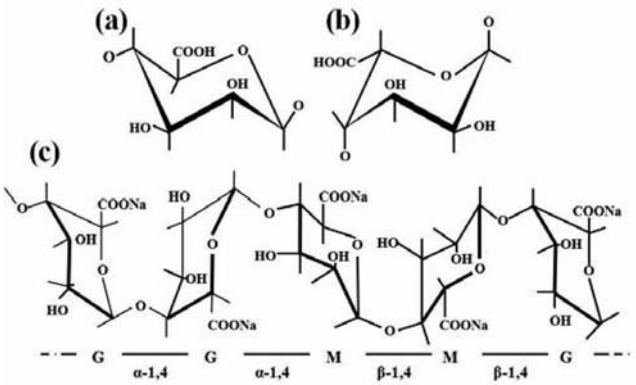

Fig. 1. Alginate composition. Alginate consists of two monomeric units. (a) β-D-mannuronic acid. (b) α-L-guluronic acid. (c) Structural formula of sodium alginate molecule.

The application of a membrane separation system in the food industry and in wastewater treatment has attracted a considerable amount of attention. Membrane separation enables process costs to be cut and results in a reduction in CO_2 emissions. In addition, interest in using natural materials has increased due to their biocompatibility and their lack of environment load upon disposal. High performance membranes made by conventional biomaterials (e.g., cellulose, [12,13] gelatin [14] and chitosan, [11,15]) were anticipated for use in biocompatible separation techniques [15].

This paper demonstrates the successful preparation of a calcium alginate membrane. The membrane preparation, mechanical strength, water content, molecular size screening, and water permeation were investigated. The membrane was sufficiently stable in an aqueous phase and exhibited not only dramatically sensitive molecular-size screening but also sufficient mechanical strength for conventional use.

2. Materials and methods

2.1. Materials

Sodium alginate of medium viscosity grade (viscosity of 10 g/l solution at 293 K, 300–400 cP) was purchased from Wako Pure Chemical Industries, Ltd. (Osaka, Japan). Its viscosity was guaranteed by the distributor. Calcium chloride (anhydrous, 95.0%), urea (60.06 Da), D(+)-glucose (180.16 Da), methyl orange (327.34 Da), and Bordeaux S (604.48 Da) were purchased from Wako Pure Chemical Industries, Ltd. (Osaka, Japan). Indigo Carmine (466.37 Da) was purchased from Kokusan Chemical Works, Ltd. (Tokyo, Japan).

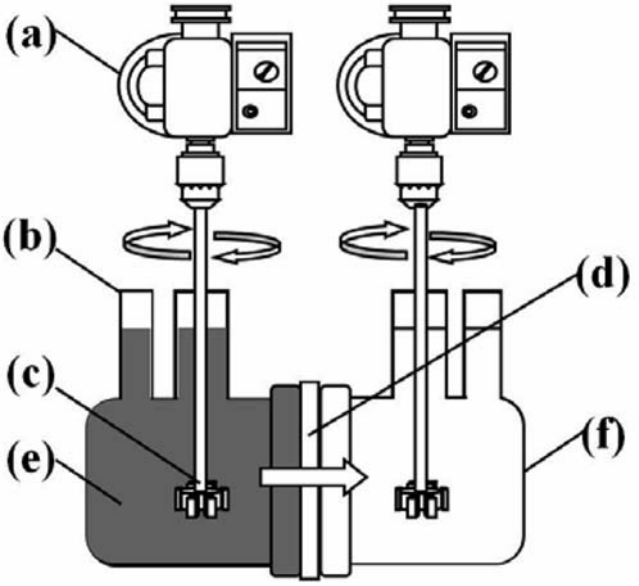

Fig. 2. Mass-transfer cells. Membrane mass transfer cells. (a) Agitating motor, (b) mass-transfer cells, (c) impeller, (d) membrane, (e) feed solution and (f) stripping solution.

2.2. Preparation of calcium alginate membrane

One gram of sodium alginate (300–400 cP, Wako) was dissolved in 100 mL of water. Calcium chloride was also dissolved in water. Its range was from 0.06 M to 1.0 M in our experiment. Twenty grams of the sodium alginate solution was dispensed on a petri dish and then completely dried in desiccators at room temperature (298 K) for one week. A dried, thin film of sodium alginate appeared on the petri dish. The calcium chloride solution was then directly introduced into it.

2.3. Mechanical strength and elastic characteristics

A wetted-state membrane sample (10 mm wide and 30 mm long) was mounted in the rheometer (CR-DX500, Sun Scientific Co., Ltd) with a crosshead speed of 2 mm/s. The maximum stress at membrane rupture was evaluated based on the load force divided by the cross-sectional area [N/m^2]. The maximum strain was evaluated as the percentage by which the length had increased at membrane rupture divided by the original length of the membrane sample.

2.4. Measurement of mass transfer flux

The overall mass transfer coefficient K_{OL} [m/s] was determined from a measurement of mass transfer flux based on Eq. (1). Twin glass mass-transfer cells sandwiched the membrane (Fig. 2). Both aqueous phases were stirred, and the cell set was installed in a thermostatic bath.

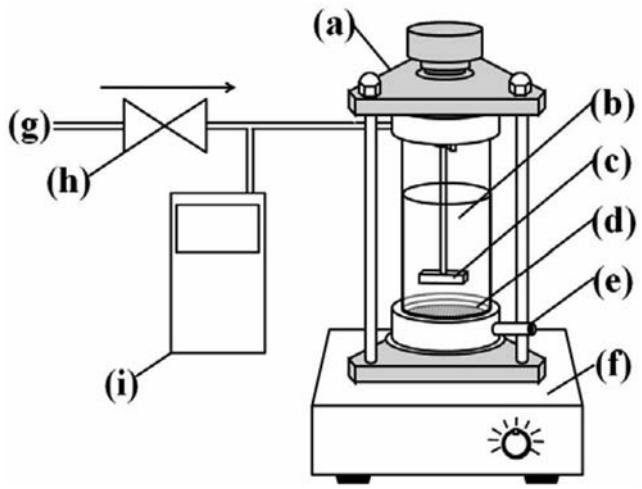

Fig. 3. Apparatus for water permeation (Model-UHP-62K. Advantec). (a) Casing frame, (b) feed water, (c) stirring bar, (d) membrane, (e) break-through point of water, (f) magnetic stirrer, (g) N_2 gas, (h) regulator valve and (i) pressure gage.

$$\ln\left(1-\frac{2C_s}{C_{fi}}\right)=-2\frac{A}{V}K_{OL}t, \tag{1}$$

$$K_{OL}^{-1}=k_{L1}^{-1}+k_m^{-1}+k_{L2}^{-1}, \tag{2}$$

The film mass-transfer resistances ${k_{L1}}^{-1}$ and ${k_{L2}}^{-1}$ in the overall mass-transfer resistance ${K_{OL}}^{-1}$ were ignored under these fully turbulent conditions. K_{OL} did not depend on the stirring rate, therefore it directly indicated the membrane mass-transfer coefficient (k_m=*Deff*/*l*/*l*) [m/s]. The effective diffusion coefficient in the membrane (*Deff*) [m^2/s] was evaluated from *km*. The membrane thickness *l* [m] was measured with a micrometer.

The concentration of the stripping solution was determined by a spectrophotometer (UV Mini 1240, Shimadzu). The absorbance of the color pigments employed (methyl orange, indigo carmine, Bordeaux S) was measured based on the maximum wavelength. The concentration of urea (glucose) was determined by the urease-indphenol method (Urea NB, Wako) (mutarotase-GOD method (Glucose C2, Wako)).

2.5. Water content

Gravimetric methods were employed to determine the water content of the membrane. The prepared membranes had already achieved the equilibrium water content. Excess water attached to the membrane surface was removed using filter paper. The mass of the swollen samples (w_e) was then measured before the wetted membrane was dried at 333 K for 24 h, and the mass of the dried membrane (w_d) was measured.

The difference between w_e and w_d indicates the mass of the total contained water (w_t).

$$w_t = w_e - w_d. \tag{3}$$

The total water content ratio (W_t) was then calculated using the following equation

$$W_t = 100\times\frac{w_e-w_d}{w_e}=100\times\frac{w_t}{w_e}. \tag{4}$$

The volume of the contained water was obtained as w_t/ρ_W. The volume of the apparent membrane in the swollen state was obtained as w_e/ρ_M. The porosity of the membrane was then calculated using the following equation

$$\varepsilon = \frac{(w_t/\rho_w)}{(w_e/\rho_M)}. \tag{5}$$

2.6. Water permeability of calcium alginate membrane

The permeability of the calcium alginate membrane was determined from the water mass flux throughput using an ultra-filtration apparatus (UHP-62K, Advantec, Tokyo). The initial volume of feed solution was a constant 200 ml. The operational pressure was adjusted by introducing nitrogen gas at room temperature (298 K). The mass of permeated water throughput was accurately measured based on the indication of an electric balance and converted to volumetric water flux by recalculation using the density of the permeated water.

2.7. Preparation of scanning electron microscopic view

The membrane was soaked in methanol to substitute for the contained water and was then dried in air (333 K, 24 h). A scanning electron microscope (Miniscope TM-1000, Hitachi) was employed.

3. Results and discussions

3.1. Measurement of mass transfer flux

Fig. 4 depicts the effect of molecular weight on membrane mass transfer. Molecular size screening was investigated by measuring the mass transfer flux in some model components. The effective diffusion coefficient in the membrane D_{eff} was changed 2.5×10^4-fold even if the molecular size was only 10-fold (Fig. 4). This remarkable size-screening effect was obtained between 60 Da (Urea) and 604 Da (Bordeaux S). It suggests that the pore size involving mass transfer was considerably monodisperse in our experiment range of molecular size. The membrane composition

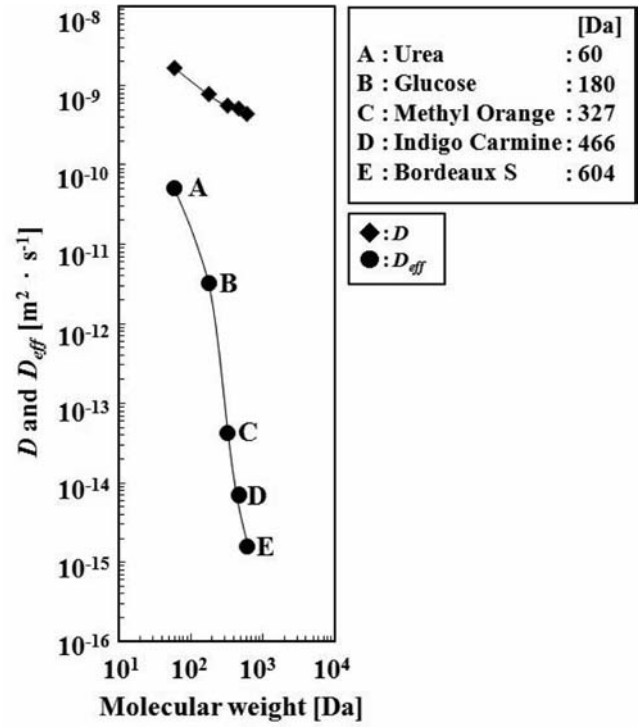

Fig. 4. Effect of molecular weight on membrane mass transfer. Temperature: 303 K. Agitation rate: 850 min^{-1}, 0.1 [mol-Ca^{2+} g-alginate^{-1}].

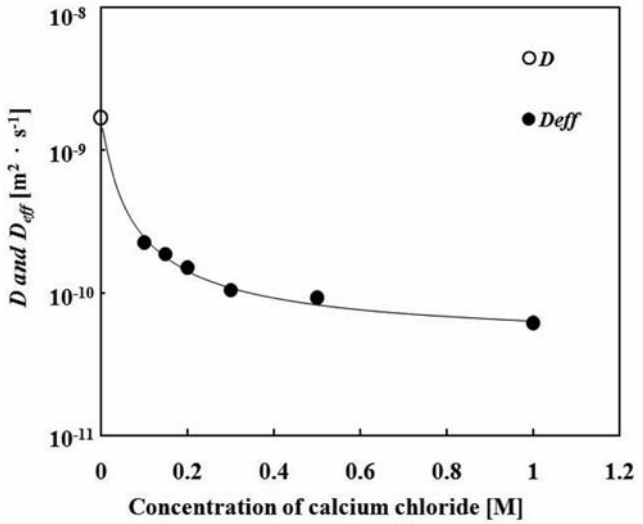

Fig. 5. Effect of calcium chloride on the effective diffusion coefficient of urea (303 K, 850 m^{-1}). Circle indicates the diffusion coefficient of urea in bulk aqueous phase.

employed in Fig. 4 was expressed conveniently as 0.1 [mol-Ca^{2+} g-alginate^{-1}], which is the molar Ca^{2+} to unit mass of alginate. In this case, the concentration of calcium chloride was fixed at 1 M. The effect of the molar ratio of Ca^{2+} to alginate polymer on the effective diffusion coefficient is very important for determining the amount of Ca^{2+} required for high performance.

The diffusion coefficient in bulk aqueous phase D was plotted for comparison. It depended on the 0.5 power of the molecular weight. In contrast, the effective diffusion coefficient depended on almost the fifth power of the molecular weight of the tested components. The membrane we used did not absorb the tested components. This was easily checked due to the color pigments employed. The large dependence of effective diffusion coefficient on molecular weight indicates that the polymeric framework of a calcium alginate membrane performs selective mass transfer based on molecular size.

Fig. 5 illustrates the effect of the calcium chloride concentration during membrane preparation on the effective diffusion coefficient of urea. The effective diffusion coefficient gradually decayed due to progressive cross-linking of molecular frameworks in the membrane. At calcium chloride concentrations over 0.1 M, the dependency of the effective diffusion coefficient on the calcium chloride concentration became small. This indicates that the molecular frameworks saturated in this range and that the effective diffusion coefficient remained almost constant. The calcium chloride acted as a cross-linker of molecular frameworks in the alginate molecular chain.

3.2. Mechanical strength and elastic characteristics

Fig. 6 depicts the correlation of the maximum stress at membrane rupture and the maximum strain with the calcium chloride concentration. The maximum stress gradually increased with increasing calcium chloride concentration as a cross-linker. In contrast, the maximum strain at membrane rupture was remarkably reduced by the addition of calcium chloride.

The polymeric framework of the calcium alginate became more densely populated with increasing calcium chloride concentration, and its mechanical strength was elevated. In our experiments, calcium chloride concentrations between 0.1 and 1.0 M were mainly employed.

Fig. 7 illustrates the correlation of the mechanical strength (maximum strain) and the effective diffusion coefficient of urea. Progress in the cross-linking of molecular frameworks resulting from a higher calcium concentration and made the membrane less elastic. Therefore, the maximum strain of the membrane decreased with increasing calcium concentration. The effective diffusion coefficient also decreased.

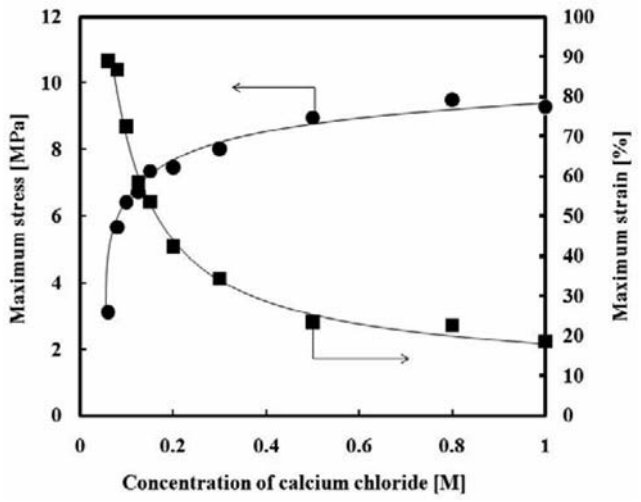

Fig. 6. Effect of the concentration of calcium chloride cross-linker on the maximum stress and strain of calcium alginate membrane. Temperature: 298 K. ●: Maximum stress. ■: Maximum strain.

3.3. Water content

Fig. 8 illustrates the effect of the concentration of calcium chloride cross-linker on the total water content of the membrane. The total water content ratio (W_t) of the calcium alginate membrane in a swelled state gradually decreased with increasing calcium chloride concentration cross-linker.

The porosity was calculated according to Eq. (5) and is presented in Fig. 9. It decreased with increasing calcium chloride concentration and approached the saturation point for cross-linking of the polymer.

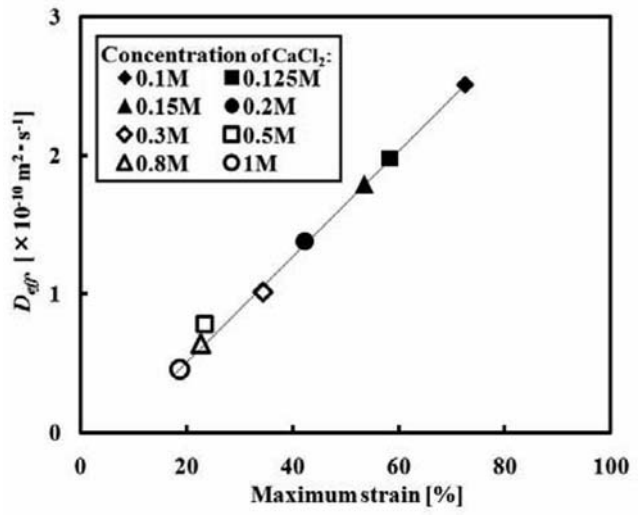

Fig. 7. Effect of the maximum strain on membrane mass transfer with urea.

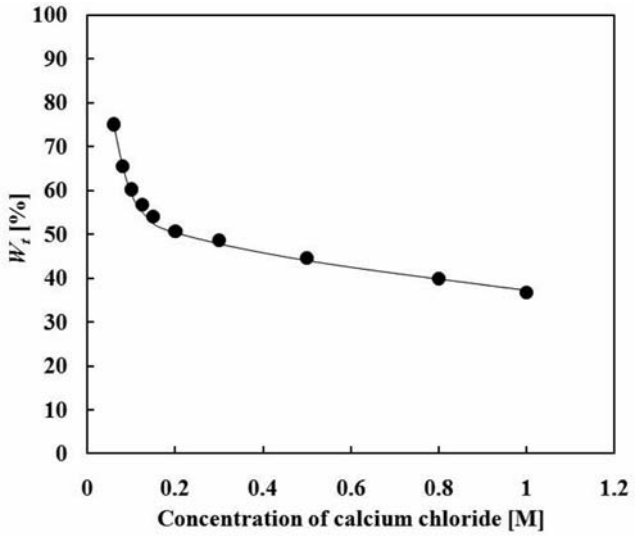

Fig. 8. Effect of the concentration of calcium chloride cross-linker on the total water content of the membrane (298 K).

3.4. Water permeability of calcium alginate membrane

The membrane was entirely hydrophilic. Fig. 10 presents the effect of operational pressure on the water flux. The water permeated throughout the membrane due to pressure, the main driving force. Water permeability was linearly proportional to the pressure. The water-permeation mechanism was assumed to be Hagen-Poiseuille flow.

Fig. 11 illustrates the effect of the concentration of the calcium chloride cross-linker on the water flux. The water permeation flux was remarkably decreased by

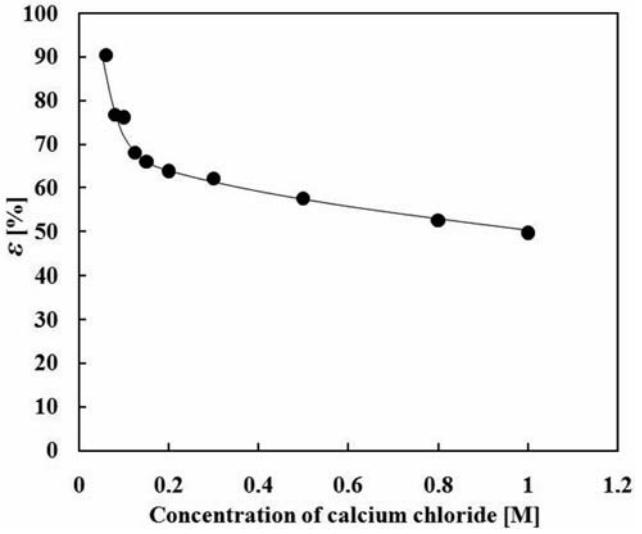

Fig. 9. Effect of concentration of calcium chloride cross-linker on membrane porosity (298 K).

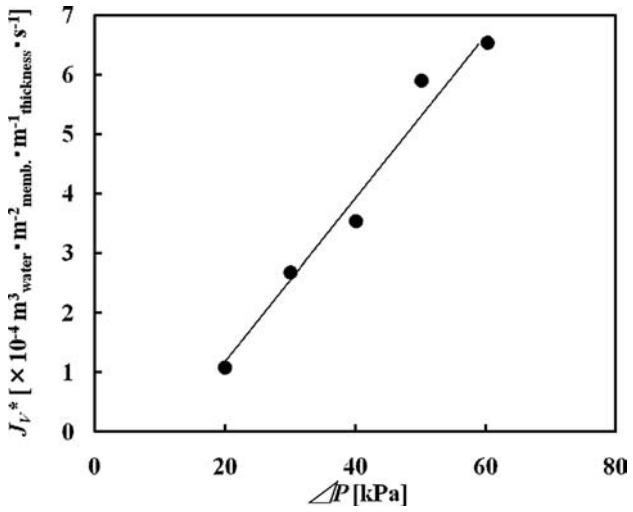

Fig. 10. Effect of operational pressure on water flux ($CaCl_2$: 0.1 M, 298 K). The water flux obeyed the Hagen–Poiseuille mechanism.

the addition of calcium chloride due to progressive cross-linking of the molecular frameworks resulting from the higher calcium concentration.

3.5. Image of scanning electron microscope

In a scanning electron microscope image, the surface of the membrane appears to be a smooth surface (Fig. 12). Pores were not observed on it. Transparent cell-like images were found on the surface.

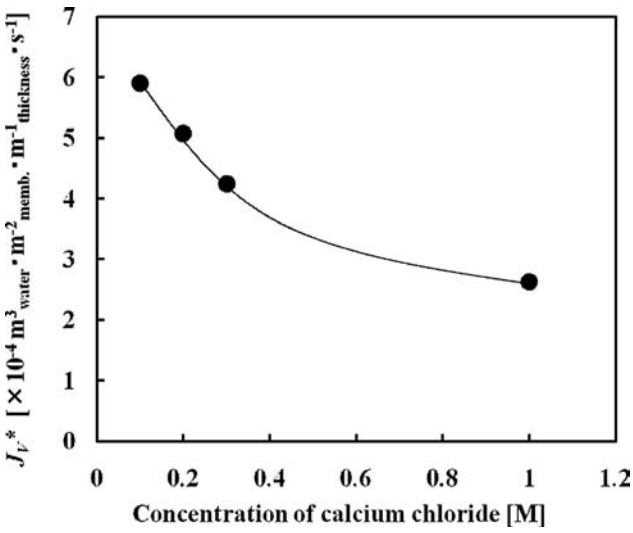

Fig. 11. Effect of the concentration of calcium chloride cross-linker on the water flux (298 K, 50 kPa).

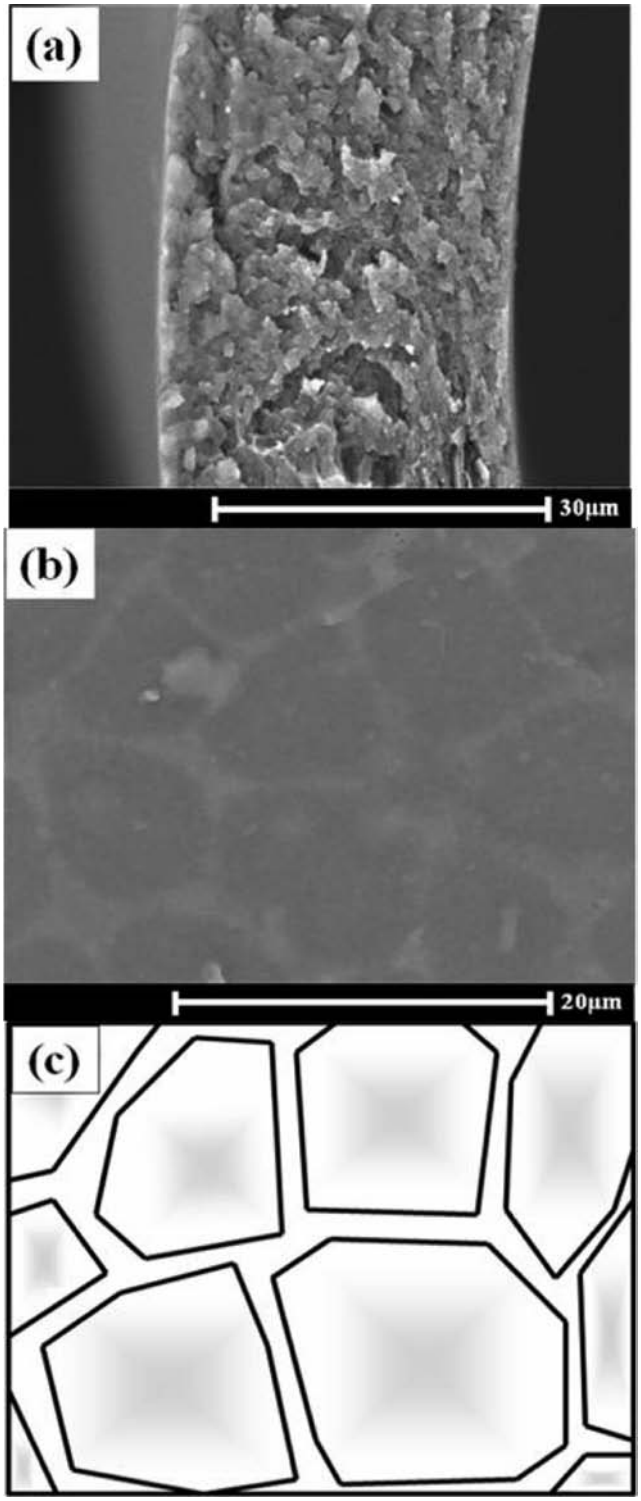

Fig. 12. SEM image of calcium alginate membranes. (a) Cross section (×3,000); (b) Cell like image was transparently found from surface (×5,000) and (c) schematic illustration of cell-like image.

4. Conclusions

A stable membrane of calcium alginate was successfully prepared. It had both superior sensitivity in molecular size screening and sufficient mechanical strength for conventional use. The polymeric framework of the calcium alginate became denser with increasing calcium chloride concentration.

Acknowledgement

The authors sincerely thank Dr. Kei Tao of Nihon University, who provided technical assistance with SEM operation and photography.

Symbols

A	Area of membrane [m^2].
C_{fi}	Initial concentration of feed solution [M].
C_s	Concentration of stripping solution [M].
D	Diffusion coefficient in bulk aqueous phase [$m\ s^{-2}$].
D_{eff}	Effective diffusion coefficient [$m\ s^{-2}$].
J_V	Water-permeated flux [$m^3_{water}\ m^{-2}_{memb.}\ s^{-1}$].
J_V^*	Water-permeated flux per unit membrane thickness, defined as (J_V/l) [$m^3_{water}\ m^{-2}_{memb.}\ m^{-1}_{thickness}\ s^{-1}$].
K_{OL}	Overall mass-transfer coefficient [$m\ s^{-1}$].
${K_{OL}}^{-1}$	Overall mass transfer resistance [$(m\ s^{-1})^{-1}$].
k_m	Membrane mass-transfer coefficient [$m\ s^{-1}$].
k_{L1}	Film mass-transfer coefficient in feed phase [$m\ s^{-1}$].
k_{L2}	Film mass-transfer coefficient in stripping phase [$m\ s^{-1}$].
l	Membrane thickness [m].
ΔP	Operational pressure [kPa].
t	Time [s].
V	Volume of aqueous solution in the transfer cell presented in Fig. 2. [m^3].
W_t	Total water content ratio [%], defined by Eq. (3).
w_e	Initial mass of the swollen membrane [kg].
w_d	Mass of dried membrane [kg].
w_t	Mass of total contained water [kg].
ε	Porosity of the membrane [%], defined by Eq. (5).
ρ_M	Density of the swollen membrane [$kg\ m^{-3}$].
ρ_W	Density of pure water [$kg\ m^{-3}$].

References

[1] T.N. Julian, G.W. Radebaugh and S.J. Wisniewski, Permeability characteristics of calcium alginate films, J. Control. Rel., 7 (1988) 165–169.
[2] S. Lee, W.S. Ang and M. Elimelech, Fouling of reverse osmosis membranes by hydrophilic organic matter: implications of water reuse, Desalination, 187 (2006) 313–321.
[3] Y. Ye, P. Le Clech, V. Chen, A.G. Fane and B. Jefferson, Fouling mechanisms of alginate solutions as model extracellular polymeric substances, Desalination, 175 (2005) 7–20.
[4] K. Katsoufidou, S.G. Yiantsions and A.J. Karabelas, Experimental study of ultrafiltration membrane fouling by sodium alginate and flux recovery by backwashing, J. Membr. Sci., 300 (2007) 137–146.
[5] P. Almeida, P. Ferreira and A.J. Almeida, Cross-linked alginate–gelatine beads: a new matrix for controlled release of pindolol, J. Control. Rel., 97 (2004) 431–439.
[6] Z. Konsoula and M. Liakopoulou-Kyriakides, Starch hydrolysis by the action of an entrapped in alginate capsules α-amylase from *Bacillus subtilis*, Process Biochem., 41 (2006) 343–349.
[7] Dembczynski, Radoslaw, and Tomasz Jankowski, Characterisation of small molecules diffusion in hydrogel-membrane liquid-core capsules, Biochem. Eng. J., 6 (2000) 41–44.
[8] G.R. Castro, R.R. Kamdar, B. Panilaitis, D.L. Kaplan, Triggered release of proteins from emulsan–alginate beads, J. Controll. Rel., 109 (2005) 149–157.
[9] J. Hubble and J.D. Newman, Alginate ultrafiltration membranes, Biotechnol. Lett., 7 (4) (1985) 273–276.
[10] C.P. Athanasekou, S.K. Papageorgiou, V. Kaselouri, F.K. Katsaros, N.K. Kakizis, A.A. Sapalidis and N.K. Kanellopoulos, Development of hybrid alginate/ceramic membranes for Cd^{2+} removal, Micropor. Mesopor. Mater., 120 (2009) 154–164.
[11] A.S. Reddya, S. Kalyani, N.S. Kumar, V.M. Boddub and A. Krishnaiah, Dehydration of 1,4-dioxane by pervaporation using crosslinked calcium alginate-chitosan blend membranes, Polym. Bull., 61 (2008) 779–790.
[12] A.M. Sokolnicki, R.J. Fisher, T.P. Harrah and D.L. Kaplan, Permeability of bacterial cellulose membranes, J. Membr. Sci., 272 (2006) 15–27.
[13] M. Zhao, X.-L. Xu, Y.-D. Jiang, W.-Z. Sun,W.-F.Wang and L.-M. Yuan, Enantioseparation of trans-stilbene oxide using a cellulose acetate membrane, J. Membr. Sci., 336 (2009) 149–153.
[14] A. Bigi, G. Cojazzi, S. Panzavolta, N. Roveri and K.Rubini, Stabilization of gelatin films by crosslinking with genipin, Biomaterials, 23 (2002) 4827–4832.
[15] T. Takahashi, M. Imai and I. Suzuki, Water permeability of chitosan membrane involved in deacetylation degree control, Biochem. Eng. J., 36 (2007) 43–48.